










## FAST Discovery of Eight Isolated Millisecond Pulsars in NGC 6517

DEJIANG YIN <sup>1</sup>, LI-YUN ZHANG <sup>1,2</sup>, LEI QIAN <sup>3,4,5,6</sup>, RALPH P. EATOUGH <sup>4,7</sup>, BAODA LI,<sup>1</sup>  
DUNCAN R. LORIMER <sup>8,9</sup>, YINFENG DAI <sup>1</sup>, YAOWEI LI,<sup>1</sup> XINGNAN ZHANG,<sup>10</sup> MINGHUI LI,<sup>10</sup>  
TIANHAO SU,<sup>1</sup> YUXIAO WU,<sup>11</sup> YU PAN,<sup>11</sup> YUJIE LIAN <sup>12,13</sup>, TONG LIU,<sup>4</sup> ZHEN YAN <sup>14</sup> AND  
ZHICHEN PAN <sup>3,4,5,6</sup>

<sup>1</sup>*College of Physics, Guizhou University, Guiyang 550025, China*

<sup>2</sup>*International Centre of Supernovae, Yunnan Key Laboratory, Kunming 650216, China*

<sup>3</sup>*Guizhou Radio Astronomical Observatory, Guizhou University Guiyang 550025, China*

<sup>4</sup>*National Astronomical Observatories, Chinese Academy of Sciences, 20A Datun Road, Chaoyang District, Beijing 100101, China*

<sup>5</sup>*CAS Key Laboratory of FAST, National Astronomical Observatories, Chinese Academy of Sciences, Beijing 100101, China*

<sup>6</sup>*College of Astronomy and Space Sciences, University of Chinese Academy of Sciences, Beijing 100049, China*

<sup>7</sup>*Max-Planck-Institut für Radioastronomie, Auf dem Hügel 69, D-53121, Bonn, Germany*

<sup>8</sup>*Department of Physics and Astronomy, West Virginia University, Morgantown, WV 26506-6315, USA*

<sup>9</sup>*Center for Gravitational Waves and Cosmology, West Virginia University, Chestnut Ridge Research Building, Morgantown, WV 26505, USA*

<sup>10</sup>*State Key Laboratory of Public Big Data, Guizhou University, Guiyang 550025, China*

<sup>11</sup>*Chongqing University of Posts and Telecommunications, Chongqing, 40000, China*

<sup>12</sup>*Institute for Frontiers in Astronomy and Astrophysics, Beijing Normal University, Beijing 102206, China*

<sup>13</sup>*Department of Astronomy, Beijing Normal University, Beijing 100875, China*

<sup>14</sup>*Shanghai Astronomical Observatory, Chinese Academy of Sciences, Shanghai 200030, China*

### ABSTRACT

We present the discovery of 8 isolated millisecond pulsars in Globular Cluster (GC) NGC 6517 using the Five-Hundred-meter Aperture Spherical radio Telescope (FAST). The spin periods of those pulsars (namely PSR J1801–0857K to R, or, NGC 6517K to R) are all shorter than 10 ms. With these discoveries, NGC 6517 is currently the GC with the most known pulsars in the FAST sky. The largest difference in dispersion measure of the pulsars in NGC 6517 is  $11.2 \text{ cm}^{-3} \text{ pc}$ , the second among all GCs. The fraction of isolated pulsars in this GC (16 of 17, 94%) is consistent with previous studies indicating an overabundance of isolated pulsars in the densest GCs, especially in those undergoing cluster core collapse. Considering the FAST GC pulsar discoveries, we modeled the GC pulsar population using the empirical Bayesian method described by Turk and Lorimer with the recent counts. Using this approach, we find that the expected number of potential pulsars in GCs seems to be correlated with the central escape velocity, hence, the GCs Liller 1, NGC 6441, M54 (NGC 6715), and  $\omega$ -Cen (NGC 5139) are expected to host the largest numbers of pulsars.

Corresponding author:

[liy\\_zhang@hotmail.com](mailto:liy_zhang@hotmail.com); [panzc@bao.ac.cn](mailto:panzc@bao.ac.cn); [lqian@nao.cas.cn](mailto:lqian@nao.cas.cn)

*Keywords:* Globular star clusters (656); Millisecond pulsars (1062); Radio telescopes (1360)

## 1. INTRODUCTION

The proportion of millisecond pulsars in Globular Clusters (GCs) with spin periods shorter than 30 ms is  $\sim 97\%$  (e.g., Yin et al. 2023), much higher than that in the field population ( $\sim 12\%^1$ ), making them rich targets for fast spinning pulsars and exotic binary systems, such as Terzan 5ad (with the highest known spin frequency of 716 Hz, Hessels et al. 2007); M4A (the triple system with a planet, Sigurdsson et al. 2003); M71E (a binary in M71 with an orbit of 53 minutes, Pan et al. 2023); M15C (a double neutron star binary, Anderson et al. 1990); and NGC 1851E (a pulsar–black hole system candidate, Barr et al. 2024). GCs have been the subject of pulsar searches for more than 30 years. Since the first GC pulsar was discovered (Lyne et al. 1987), 322 radio pulsars have been detected in 41 GCs as of May 2023<sup>2</sup>. Previous surveys for GC pulsars have been carried out with telescopes across the world, including Lovell (e.g., Lyne et al. 1987), Parkes (e.g., Robinson et al. 1995), Arecibo (e.g., Hessels et al. 2007), Green Bank Telescope (GBT, e.g., Ransom et al. 2005), and Giant Metrewave Radio Telescope (GMRT, e.g., Gautam et al. 2022).

In the past 5 years alone, about 120 GC pulsars have been discovered with newly built telescopes. MeerKAT (Jonas & MeerKAT Team 2016) found  $\sim 80$  GC pulsars (e.g., Ridolfi et al. 2021, TRAPUM project<sup>3</sup>) and the telescope used in this work, Five-hundred-meter Aperture Spherical radio Telescope (FAST, Nan et al. 2011) discovered another  $\sim 40$  (e.g., Pan et al. 2020, FAST GC Pulsar Discoveries<sup>4</sup>). With a sensitivity limit of  $4 \mu\text{Jy}$ , 100 to 300 GC pulsars are expected to be discovered by SKA1-MID when it comes online (Hessels et al. 2015).

Among 170 Galactic GCs, there are 45 in the FAST sky. One of these 45 GCs, NGC 6517 is located at  $\alpha_{\text{J2000}} = 18^{\text{h}}01^{\text{m}}50.52^{\text{s}}$ ,  $\delta_{\text{J2000}} = -08^{\circ}57'31.6''$ . It is the densest GC ( $\rho_0 = 10^{5.29} L_{\odot} \text{pc}^{-3}$ ) in the FAST sky. Its core and half-light radius are  $r_c = 0.06'$  and  $r_h = 0.50'$ , respectively (Harris 1996, 2010 edition), well within the FAST half-power beamwidth at L-band ( $\sim 2.9'$ , Qian et al. 2020). The four pulsars, PSR J1801–0857A to D (NGC 6517A to D), were detected by the GBT (Lynch et al. 2011). The dispersion measures (DMs) of those pulsars range from 174.71 to 182.56  $\text{cm}^{-3} \text{pc}$ . PSR J1801–0857E, F, and G (NGC 6517E, F, and G) were discovered by FAST with a candidate selection method based on DM–signal-to-noise ratio curves (Pan et al. 2021a). PSR J1801–0857H and I (NGC 6517H and I) were also discovered at FAST in long tracking observations (Pan et al. 2021b). Currently, NGC 6517B is the only binary pulsar ( $\sim 60$  d orbital period) detected in this GC. Among all 41 GCs currently known to host pulsars, NGC 6517 ranks third highest in terms of the fraction of isolated pulsars, at 94%. Only NGC 6522, where 6 out of the 6 known pulsars are isolated, and Terzan 1 (8 out of 8) have a higher fraction. This is in spite of the fact that, as described below, our analyses of NGC 6517 include acceleration searches which aim to retain sensitivity to binary systems.

Located at 10.4 and 10.6 kpc away from the Sun (Harris 1996, 2010 edition), NGC 6517 and M15 (NGC 7078) respectively, are the only two core-collapsed GCs (e.g., Verbunt & Freire 2014) in

<sup>1</sup> Manchester et al. 2005, 1.70 version, <https://www.atnf.csiro.au/people/pulsar/psrcat/>

<sup>2</sup> <https://www3.mpifr-bonn.mpg.de/staff/pfreire/GCpsr.html>

<sup>3</sup> <http://trapum.org/discoveries/>

<sup>4</sup> <https://fast.bao.ac.cn/cms/article/65/>

the FAST sky. The isolated pulsars in NGC 6517 and M15 dominate the pulsar population, similar to other core-collapsed GCs outside the FAST sky, such as Terzan 1 (8 isolated, 0 binaries) and NGC 6624 (10 isolated, 2 binaries). In [Verbunt & Freire \(2014\)](#) a dynamical parameter, the encounter rate per binary in a GC,  $\gamma$  ( $\gamma \propto \rho_0^{0.5} r_c^{-1}$ ,  $\rho_0$  is the central mass density and  $r_c$  is the core radius), was used as a factor to characterize the differences between the pulsar populations of different GCs. Original millisecond pulsar binaries are thought to be disrupted by an exchange encounter, enabled by the higher  $\gamma$  in core-collapsed clusters. The high fraction of isolated pulsars in core-collapsed GCs is therefore a natural result of the increased number of these encounter and disruption events. In addition, several alternative formation scenarios are proposed to explain the seeming overabundance of isolated millisecond pulsars in core-collapsed clusters, such as the formation of single millisecond pulsars via accretion following mergers of neutron stars and main-sequence stars (e.g., [Davies et al. 1992](#); [Camilo & Rasio 2005](#); [Kremer et al. 2022](#)), the formation of single pulsars via mergers of massive white dwarf binaries (e.g., [King et al. 2001](#); [Schwab 2021](#); [Kremer et al. 2023](#)), and the number of single millisecond pulsars in GCs can significantly be boosted by both main-sequence star tidal disruption events and merger-induced collapses discussed in the recent N-body simulations ([Ye et al. 2024](#)).

Ranking third among the GCs with the most pulsars in the FAST sky, NGC 6517 is one of pulsar search targets with the highest chance for further discoveries (see, e.g., [Turk & Lorimer 2013](#)). Motivated by this potentially significant pulsar population, in this work we present the discovery of an additional eight pulsars in NGC 6517, bringing the total number to 17 in this cluster. The new discoveries were made during the reprocessing of FAST archival data and increase the total number of GC pulsars discovered by FAST to 49. Pulsar population simulations can help to predict the expected number of GC pulsars. Due to sensitivity limits and the selection effects of binary pulsar search algorithms, the number of known pulsars in a given GC can be much lower than predictions from simulations. The stellar encounter rate  $\Gamma$ , which is estimated with  $\Gamma \propto \rho_0^{1.5} r_c^2$  ( $\rho_0$  is the central mass density and  $r_c$  is the core radius, [Pooley et al. 2003](#)), has also been used to estimate the GC pulsar numbers (e.g., [Pooley et al. 2003](#); [Abdo et al. 2009](#)). The number of potential pulsars in a GC is scaled by its  $\Gamma$  in the empirical Bayesian model of [Turk & Lorimer \(2013\)](#). This method was used to estimate the total population of pulsars for all Galactic GCs and predicted a number of  $2280_{-1490}^{+2720}$  ([Turk & Lorimer 2013](#)). In light of the number of GC pulsars discovered by FAST, it is timely to revisit the population analysis carried out a decade ago by [Turk & Lorimer \(2013\)](#).

The observations and data reduction are presented in Section 2. The discoveries of pulsars and their timing solutions are given in Section 3. Section 4 provides an updated analysis of the pulsar population in GCs using the procedures described in [Turk & Lorimer \(2013\)](#). A summary of the findings is given in Section 5.

## 2. OBSERVATIONS AND DATA REDUCTION

### 2.1. Observations

As a part of the project ‘‘Globular Cluster FAST: A Neutron-star Survey’’ (GC FANS, [Pan et al. 2021b](#); [Wu et al. 2023](#)), the first observation of NGC 6517 was performed on June 24, 2019. By December 31, 2022, a total of 19 observations with integration lengths between 1400 s and 9000 s were carried out. The data were taken with the central beam of the FAST 19-beam receiver covering a frequency range of 1.0-1.5 GHz. The data were channelized into 4096 channels (channel

width 0.122 MHz). All observations were performed with the tracking mode with a sampling time of  $49.152 \mu\text{s}$  and packaged into the standard search-mode PSRFITS data format (Hotan et al. 2004). During each observation, the central beam was pointed at the center of NGC 6517.

## 2.2. Data Reduction

PRESTO<sup>5</sup> (Ransom 2001; Ransom et al. 2002) and TEMPO<sup>6</sup> (Nice et al. 2015) were used for pulsar search and timing respectively. In the following, we first describe the pulsar search procedure, followed by the timing analysis.

The routine `rfifind` from PRESTO was used to identify and mask the detrimental effects of terrestrial radio frequency interference (RFI) in both the time and frequency domains. The `prepdata` or `prepsubband` routines were used to dedisperse the PSRFITS data over a range of trial DM values. Since the DM of previously known pulsars in NGC 6517 ranges from  $174.7 \text{ cm}^{-3} \text{ pc}$  (NGC 6517D) to  $185.6 \text{ cm}^{-3} \text{ pc}$  (NGC 6517G), with an average of  $181.3 \text{ cm}^{-3} \text{ pc}$ , dedispersion was performed across a DM range of 170 to  $190 \text{ cm}^{-3} \text{ pc}$ , with a step of  $0.05 \text{ cm}^{-3} \text{ pc}$ . This DM coverage was determined to maintain sensitivity to any undiscovered pulsars in NGC 6517.

To identify periodic signals, the dedispersed time series were transformed into the fluctuation frequency domain using the routine `realfft`. The routine `accelsearch` was then used to perform Fourier domain acceleration searches, with harmonic summing to account for pulses of narrow duty cycle. The `accelsearch` parameter `zmax` represents the largest drift of the pulse frequency, in Fourier bins, under the assumption of a constant acceleration (Ransom et al. 2002). We performed a search for isolated pulsars with a `zmax` of 20 and a segmented acceleration search (with time series of length down to 1/5 of the original integration time which ranged from 500 s to 1800 s) for binaries and with a `zmax` of 1200.

So-called candidate “sifting” routines were then used to amalgamate multiple detections of each pulsar candidate from the `accelsearch` results. Both the routine `ACCEL_sift.py` of PRESTO and `JinglePulsar`<sup>7</sup> were used for this task. We also identified any candidates that appeared on different days, but with similar spin period and DM values. This method will be described in another publication (Yu et al., in preparation).

In the final stage of the pulsar search, the `prepfold` routine was used to fold all sifted pulsar candidates using either dedispersed time series, or raw PSRFITS data, to generate standard pulsar candidate diagnostic plots for visual inspection.

The timing analysis of detected pulsars was performed as follows:

1. The observational data were dedispersed to time series according to the candidate DM value. During this process, the RFI “mask” generated earlier from the routine `rfifind` was used.
2. The dedispersed and RFI cleaned time series were folded at the pulsar spin period in the topocentric reference frame by the routine `prepfold`.
3. The PRESTO routines `pygaussfit.py` and `get_TOAs.py` were utilized to form a standard reference template profile and extract the times of arrival (TOAs), respectively.

<sup>5</sup> <https://github.com/scottransom/presto>

<sup>6</sup> <http://nanograv.github.io/tempo/>

<sup>7</sup> <https://github.com/jinglepulsar/jinglesifting>

4. The initial pulsar ephemeris was then iterated using TEMPO over progressively longer time spans until a phase-connected timing solution was obtained.

A phase-connected timing solution means that every rotation of the pulsar can be accurately predicted by an ephemeris. The `pyplotres.py` routine from PRESTO was used to realize interactive inspection of timing residuals. The ephemerides of pulsars were gradually fitted and updated by removing the arbitrary phase offsets (with so-called “JUMPs”) between epochs. In the archival observations of NGC 6517, the gap between observations could be up to more than one year. The script `Dracula`<sup>8</sup> was also used to determine the exact rotation count of pulsars (Freire & Ridolfi 2018).

### 3. RESULTS

Eight isolated millisecond pulsars in NGC 6517, namely PSR J1801–0857K to R (NGC 6517K to R)<sup>9</sup>, were discovered during the reprocessing of FAST archival data. The same data set was used to time these newly discovered pulsars and the other known pulsars in NGC 6517. Our discoveries make NGC 6517 the GC with the most known pulsars in the FAST sky, hosting a total of 17 pulsars. The spin periods of the new pulsars are all shorter than 10 ms. Their pulse profiles and timing residuals are in Figure 1. The timing solution of NGC 6517B, the only known binary in the GC, was obtained with the “BT” model (Blandford & Teukolsky 1976), which includes the projected pulsar semi-major axis ( $x_p$ ), eccentricity ( $e$ ), epoch of periastron passage ( $T_0$ ), orbital period ( $P_b$ ) and longitude of periastron passage ( $\omega$ ).

**Table 1.** The timing solutions of known pulsars NGC 6517A to I and new pulsars NGC 6517K to O. In the timing analysis, the DE438 Solar System Ephemeris and the TBD time units are used and the times were not referenced to one of the atomic time standards (UNCORR). The timing data spans from MJD 58659 to 59944 for NGC 6517A to M, MJD 58688 to 59944 for NGC 6517N and NGC 6517O.

Pulsar	J1801–0857A	J1801–0857B	J1801–0857C
Right ascension, $\alpha$ (J2000) .....	18:01:50.61097(7)	18:01:50.5654(1)	18:01:50.73891(5)
Declination, $\delta$ (J2000) .....	−08:57:31.905(3)	−08:57:32.867(7)	−08:57:32.761(3)
Spin frequency, $f$ ( $s^{-1}$ ) .....	139.36088855893(2)	34.52849284047(2)	267.47267670678(3)
1st spin frequency derivative, $\dot{f}$ ( $Hz\ s^{-2}$ )	$9.9034(4)\times 10^{-15}$	$-2.6270(2)\times 10^{-15}$	$4.5058(8)\times 10^{-15}$
Reference epoch (MJD) .....	58871.058570	58871.058570	58871.058570
Dispersion measure, DM ( $pc\ cm^{-3}$ ) .....	182.655(3)	182.402(3)	182.356(2)
Number of TOAs .....	149	152	150
Post-fit residual RMS ( $\mu s$ ) .....	17.78	25.10	15.15
Binary Parameters			
Binary model .....	–	BT	–
Projected semi-major axis, $x_p$ (lt-s) .....	–	33.87542(1)	–

Continued on next page

<sup>8</sup> <https://github.com/pfreire163/Dracula>

<sup>9</sup> The previously announced pulsar NGC 6517J, was subsequently identified as the 17<sup>th</sup> spin frequency harmonic of NGC 6517B.

Table 1 – Continued from previous page

Orbital eccentricity, $e$ .....	–	$3.82259(6) \times 10^{-2}$	–
Longitude of periastron, $\omega$ (deg) .....	–	$-57.8927(7)$	–
Epoch of periastron passage, $T_0$ (MJD) .	–	$54757.7229(1)$	–
Orbital period, $P_b$ (days) .....	–	$59.8364531(8)$	–
Derived Parameters			
Spin period, $P$ (ms) .....	$7.175614409039(1)$	$28.96158846609(1)$	$3.7386996395757(5)$
1st Spin period derivative, $\dot{P}$ ( $\text{s s}^{-1}$ ) ....	$-5.0992(2) \times 10^{-19}$	$2.2034(2) \times 10^{-18}$	$-6.298(1) \times 10^{-20}$
Derived Parameters			
<b>Pulsar</b>	<b>J1801–0857D</b>	<b>J1801–0857E</b>	<b>J1801–0857F</b>
Right ascension, $\alpha$ (J2000) .....	$18:01:55.36430(7)$	$18:01:50.6240(1)$	$18:01:50.7417(1)$
Declination, $\delta$ (J2000) .....	$-08:57:24.316(3)$	$-08:57:31.331(8)$	$-08:57:31.292(8)$
Spin frequency, $f$ ( $\text{s}^{-1}$ ) .....	$236.60059797388(3)$	$131.55003246018(5)$	$40.17357389120(1)$
1st Spin frequency derivative, $\dot{f}$ ( $\text{Hz s}^{-2}$ )	$-4.211(8) \times 10^{-16}$	$1.7928(1) \times 10^{-14}$	$4.3105(3) \times 10^{-15}$
Reference Epoch (MJD) .....	$58871.058570$	$58871.058570$	$58871.058570$
Dispersion measure, DM ( $\text{pc cm}^{-3}$ ) .....	$174.537(3)$	$183.184(5)$	$183.785(5)$
Number of TOAs .....	151	146	152
Post-fit residual RMS ( $\mu\text{s}$ ) .....	17.36	40.32	34.35
Derived Parameters			
Spin period, $P$ (ms) .....	$4.2265320061042(6)$	$7.601670492196(3)$	$24.891985032456(8)$
1st Spin period derivative, $\dot{P}$ ( $\text{s s}^{-1}$ ) ....	$7.52(1) \times 10^{-21}$	$-1.03598(6) \times 10^{-18}$	$-2.6708(2) \times 10^{-18}$
Derived Parameters			
<b>Pulsar</b>	<b>J1801–0857G</b>	<b>J1801–0857H</b>	<b>J1801–0857I</b>
Right ascension, $\alpha$ (J2000) .....	$18:01:50.0979(7)$	$18:01:52.5989(2)$	$18:01:53.5073(2)$
Declination, $\delta$ (J2000) .....	$-08:57:27.53(3)$	$-08:57:45.04(1)$	$-08:57:41.84(1)$
Spin frequency, $f$ ( $\text{s}^{-1}$ ) .....	$19.38308799410(3)$	$177.21938880576(8)$	$307.2974449774(2)$
1st Spin frequency derivative, $\dot{f}$ ( $\text{Hz s}^{-2}$ )	$-4.01(7) \times 10^{-17}$	$-1.078(2) \times 10^{-15}$	$1.550(4) \times 10^{-15}$
Reference epoch (MJD) .....	$58871.058570$	$58871.058570$	$58871.058570$
Dispersion measure, DM ( $\text{pc cm}^{-3}$ ) .....	$185.06(2)$	$179.634(9)$	$177.877(9)$
Number of TOAs .....	145	141	70
Post-fit residual RMS ( $\mu\text{s}$ ) .....	136.77	49.96	34.58
Derived Parameters			
Spin period, $P$ (ms) .....	$51.59136667513(8)$	$5.642723444307(3)$	$3.254176096627(2)$
1st Spin period derivative, $\dot{P}$ ( $\text{s s}^{-1}$ ) ....	$1.07(2) \times 10^{-19}$	$3.431(6) \times 10^{-20}$	$-1.642(4) \times 10^{-20}$
Derived Parameters			
<b>Pulsar</b>	<b>J1801–0857K</b>	<b>J1801–0857L</b>	<b>J1801–0857M</b>
Right ascension, $\alpha$ (J2000) .....	$18:01:50.7212(9)$	$18:01:49.5847(7)$	$18:01:50.6297(4)$
Declination, $\delta$ (J2000) .....	$-08:57:32.56(4)$	$-08:57:08.06(4)$	$-08:57:31.45(2)$
Spin frequency, $f$ ( $\text{s}^{-1}$ ) .....	$104.2699714144(2)$	$165.0902463911(2)$	$186.6773548929(1)$

Continued on next page

Table 1 – Continued from previous page

1st Spin frequency derivative, $\dot{f}$ (Hz s <sup>-2</sup> )	$-8.893(4)\times 10^{-15}$	$9.21(6)\times 10^{-16}$	$-1.6932(3)\times 10^{-14}$
Reference epoch (MJD)	58868.079260	58867.093100	58871.058500
Dispersion measure, DM (pc cm <sup>-3</sup> )	182.38(2)	185.74(2)	183.18(1)
Number of TOAs	54	60	59
Post-fit residual RMS ( $\mu$ s)	108.18	93.82	55.52
Derived Parameters			
Spin period, $P$ (ms)	9.59048886688(2)	6.057293037354(9)	5.356836133518(4)
1st Spin period derivative, $\dot{P}$ (s s <sup>-1</sup> )	$8.180(3)\times 10^{-19}$	$-3.38(2)\times 10^{-20}$	$4.8586(9)\times 10^{-19}$
<b>Pulsar</b>	<b>J1801–0857N</b>	<b>J1801–0857O</b>	
Right ascension, $\alpha$ (J2000)	18:01:50.6318(5)	18:01:50.7720(3)	
Declination, $\delta$ (J2000)	-08:57:34.50(2)	-08:57:33.37(2)	
Spin frequency, $f$ (s <sup>-1</sup> )	200.2170232280(2)	233.2571878284(2)	
1st Spin frequency derivative, $\dot{f}$ (Hz s <sup>-2</sup> )	$2.1306(5)\times 10^{-14}$	$-7.149(4)\times 10^{-15}$	
Reference epoch (MJD)	58868.079200	59941.134200	
Dispersion measure, DM (pc cm <sup>-3</sup> )	182.642(9)	182.49(1)	
Number of TOAs	57	54	
Post-fit residual RMS ( $\mu$ s)	68.11	46.74	
Derived Parameters			
Spin period, $P$ (ms)	4.994580300304(5)	4.287113333183(4)	
1st Spin period derivative, $\dot{P}$ (s s <sup>-1</sup> )	$-5.315(1)\times 10^{-19}$	$1.3139(8)\times 10^{-19}$	

**Table 2.** The information of NGC 6517P, Q, R from preliminary timing measurements made to date. The timing data spans from MJD 58689, 58867 and 58856 to 59944 for NGC 6517P, Q and R, respectively. The optical center of NGC 6517 is used as the pulsar’s position. The  $\dot{f}$  of each pulsar is fixed to 0.

<b>Pulsar</b>	<b>J1801–0857P</b>	<b>J1801–0857Q</b>	<b>J1801–0857R</b>
Spin frequency, $f$ (s <sup>-1</sup> )	180.632266(2)	137.776526(2)	151.8545784(9)
Reference epoch (MJD)	59944.125910	58871.058570	59944.125910
Dispersion measure, DM (pc cm <sup>-3</sup> )	183.05	182.45	182.50
Number of TOAs	33	24	29
Post-fit residual RMS ( $\mu$ s)	119.84	91.53	56.03
Derived Parameters			
Spin period, $P$ (ms)	5.53610949(6)	7.25813048(9)	6.58524762(4)

Whilst obtaining or updating the timing solutions for all known pulsars in (NGC 6517A to I) we find solutions that are consistent with previous studies (Lynch et al. 2011; Pan et al. 2021a), albeit

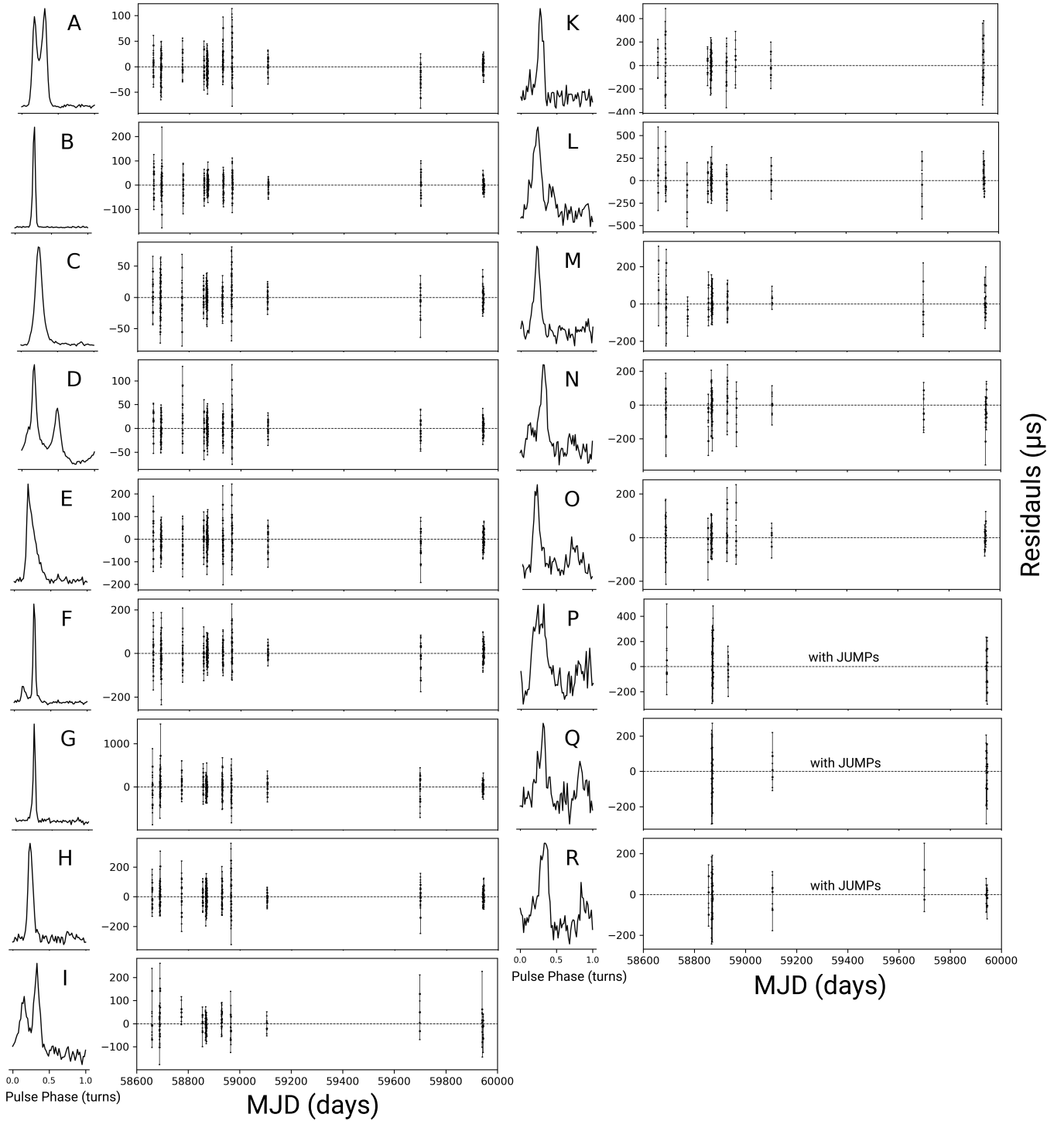


**Figure 1.** The average pulse profiles and timing residuals of all pulsars in NGC 6517. The left panel of each subplot is the integrated pulse profile obtained by summing all detections over 64 pulse phase bins. The timing residuals from the best-fit timing model are shown in the right panel. The phase-connected timing solutions of NGC 6517A to O were obtained, while for NGC 6517P, Q, and R, solutions with only the spin frequencies ( $f$ ) were fitted, with commonly used arbitrary phase offsets (so-called “JUMPs”) between observations.



with measurements of higher precision (e.g.,  $\alpha$  and  $\delta$  were improved in their accuracy by at least one decimal place). Of the newly discovered pulsars, we can only obtain the phase-connected timing solutions for NGC 6517K, L, M, N, and O. The phase-connected timing solutions of NGC 6517A to M were obtained by manually removing the JUMPs between different observations. For the pulsars NGC 6517N and O, the *Dracula* algorithm returned single solutions with a reduced  $\chi^2 < 2$ . Presently, only NGC 6517B is confirmed as a binary pulsar and the other pulsars appear to be isolated. Updated timing solutions for all previously known pulsars in NGC 6517, in addition to solutions for the newly discovered pulsars described in this work, are presented in Table 1. For the other three pulsars, NGC 6517P, Q, and R, their low flux density ( $S_{\text{mean}} \sim 1 \mu\text{Jy}$ ) led to intermittent detection through standard search methods. However, once the observations were folded with a basic ephemeris containing the spin period, and adopting the central location of NGC 6517 as the pulsar position, detections could be made in all observations longer than  $\sim 2$  h. Continuous monitoring to increase the number of detections of PSRs NGC 6517P, Q, and R is needed to remove JUMPs (see Table 2 and Figure 1). Since the submission of this letter, three weaker millisecond pulsars, NGC 6517S to U, were detected in this cluster. Their spin periods are 3.77 ms, 3.68 ms, and 6.02 ms, respectively, and more details will be discussed in another works (Dai et al. in preparation).

Our fits for DM, including the newly discovered pulsars, show that the difference between the maximum and minimum DM of pulsars in NGC 6517 is  $\sim 11.2 \text{ cm}^{-3} \text{ pc}$ , making it the GC with the second largest spread in pulsar DMs. Only GLIMPSE-C01, with pulsars that show a DM range of  $\sim 62 \text{ cm}^{-3} \text{ pc}$ , is larger. The DM difference may be caused by the intrinsic nature of the interstellar medium (ISM) within GCs, or the turbulent nature of the Galactic ISM on small angular scales (see e.g., Freire et al. 2005). NGC 6517, located close to the Galactic plane, is therefore a useful yardstick for understanding these effects. Three X-ray sources were detected in 0.3-8 keV with luminosities ranging from  $2.7 \times 10^{31} \text{ erg s}^{-1}$  to  $2.4 \times 10^{32} \text{ erg s}^{-1}$  (Zhao & Heinke 2022). Because nine of the 17 pulsars lie within the core-radius, their possible association with X-ray counterparts will be discussed in another paper (Yin et al. in preparation).

#### 4. AN UPDATE ON THE ESTIMATED NUMBER OF GC PULSARS

After making the first detections of pulsars in NGC 6517, Lynch et al. (2011) made complete population predictions for this GC using three observed pulsar luminosity functions, and with limits defined by the peak luminosity of the pulsars detected and the weakest known GC pulsar at that time. They found that 12 to 17 pulsars would exist in this GC. We note the upper limit from Lynch et al. (2011) now matches the known pulsar population in NGC 6517, however, as discussed below, the new pulsar discoveries described in this work change population predictions. Since then other methods have been employed that not only predict the number of pulsars in GCs such as NGC 6517, but try to establish possible correlation between the intrinsic cluster properties and their pulsar count (Turk & Lorimer 2013). The empirical Bayesian method described by Turk & Lorimer (2013) was designed to model pulsar populations that are heavily biased by selection effects resulting in populations with either low to zero pulsar detections. For NGC 6517 this method results in a prediction of  $\sim 15$  pulsars.

Using the publicly available software<sup>10</sup> described in Turk & Lorimer (2013) it was found that by incorporating recent pulsar discoveries from FAST, the predicted number of pulsars using this method

<sup>10</sup> <http://astro.phys.wvu.edu/gcpsrs/empbayes>

in GCs M53 and M71 differed from earlier estimations by 3 to 14 and 1 to 4 pulsars respectively. Because all GCs in the FAST sky have now been searched for undiscovered pulsars, resulting in a total of 50 new discoveries<sup>11</sup>, in this work we used the updated detected pulsar count, including FAST detections, to re-evaluate the optimal models found using the method described by Turk & Lorimer (2013). As this method can be used to investigate the largely unknown relationship between GC properties and their pulsar population, incorporating the increased pulsar sample is expected to elucidate this further.

We applied largely the same methods as outlined in Turk & Lorimer (2013), and refer the reader to this work for detailed descriptions of the statistical methods used. In the following, only the necessary definitions have been explained. The GC parameters to be investigated included the optical  $V$ -band luminosity ( $L_V$ ); escape velocity ( $V_{\text{esc}}$ ); metallicities ( $M_L$ ) from Harris 1996 (2010 edition); stellar encounter rates ( $\Gamma$ ) from Bahramian et al. (2013); and minimum detectable flux densities ( $S_{\text{min}}$ ) from Boyles et al. (2011). In Turk & Lorimer (2013) a total of 94 GCs (with 144 known pulsars in 28 of the GCs) with all five of these parameters measured were used. An a-priori candidate set of 240 models,  $\hat{N}_{\text{psr},i}$ , were modelled with different covariate effects,  $X_{ij}$ , which are combinations of the physical properties of the GCs mentioned above and their regression coefficients,  $\beta_i$ . Here  $X_{ij}$  is the  $j^{\text{th}}$  covariate in  $i^{\text{th}}$  GC ( $j = 1, 2, \dots, r$ ) and the regression coefficient  $\beta_j$  characterises the effect of the  $j^{\text{th}}$  covariate. These were then evaluated by the Akaike's Information Criterion (AIC, Burnham & Anderson 2004) to select optimal models; where models with smaller AIC values (by at least two AIC units, Burnham & Anderson 2004) are considered to provide a better fit to the sample data. In Turk & Lorimer (2013) the estimated detection probability,  $\hat{p}_i$ , for the  $i^{\text{th}}$  GC was considered in three prior distributions on GC pulsar population ( $\hat{N}_{\text{psr},i}$ ): Poisson (P), negative binomial (NB), and zero-inflated Poisson (ZIP). Through their analysis Turk & Lorimer (2013) found that the stellar encounter rate is the most critical parameter in estimating the number of pulsars in a GC.

In our updated analysis we divided the GC samples into two groups. Firstly we fitted models using all 94 GCs, but with updated pulsar counts. Our second sample consisted of only the GCs visible from FAST. The reasoning for this is described below. For the first sample of all 94 GCs, the results from the AIC ranking showed that models which included escape velocity were favored over models in which this was not a factor. The results from the most simplified models (i.e., those with the fewest parameters) within 2 AIC units are shown in the upper section of Table 3. The second sample of FAST only GCs was chosen for the following reasons. To date, almost all GCs within the FAST sky have been deeply searched for pulsars (limiting flux of  $\sim 1 \mu\text{Jy}$ , Pan et al. 2021b) by FAST. The searches for GC pulsars outside the FAST sky have been carried out by different telescopes with different sensitivity and observing systems. Therefore we assume that a sample with uniform sensitivity coverage could reduce the influence of selection bias and more accurately reveal the underlying distribution of the pulsar population in GCs.

There are 45 GCs in the FAST sky and amongst these, 31 were used because they have all five of the necessary GC property parameters. Results from the three models most highly ranked by their AIC values are presented in the lower section of Table 3. For our GC sample covering the FAST sky, models which included the GC escape velocity  $V_{\text{esc}}$  are also favored over other models in which this is not a factor. The AIC values of the three models in the lower section of Table 3 are almost equal.

<sup>11</sup> <https://fast.bao.ac.cn/cms/article/65>

**Table 3.** The top models within two AIC units to the smallest AIC.  $\Delta\text{AIC}$  is the change in AIC relative to the model with smallest AIC value and Type refers to the model prior used for abundance, in this case Negative Binomial (NB), see Turk & Lorimer (2013) for details. The models in the upper section are from all GCs, and the results in the lower section are from GCs within the FAST sky. Note the AIC value can only be used to rank models within the same sample, not between different samples.

The sample of all GCs					
Model no.	Model Structure	AIC	$\Delta\text{AIC}$	Type	
1.	$\ln \hat{N}_{\text{psr},i} = \beta_0 + \beta_1 V_{\text{esc}} + \lg(\hat{p}_i)$	313.65	0.37	NB	
2.	$\ln \hat{N}_{\text{psr},i} = \beta_0 + \beta_1 V_{\text{esc}} + \hat{p}_i$	314.16	0.88	NB	
3.	$\ln \hat{N}_{\text{psr},i} = \beta_0 + \beta_1 V_{\text{esc}}$	314.60	1.32	NB	
The sample of only GCs within FAST sky.					
1.	$\ln \hat{N}_{\text{psr},i} = \beta_0 + \beta_1 V_{\text{esc}} + \hat{p}_i$	103.84	0.000	NB	
2.	$\ln \hat{N}_{\text{psr},i} = \beta_0 + \beta_1 V_{\text{esc}}$	103.88	0.035	NB	
3.	$\ln \hat{N}_{\text{psr},i} = \beta_0 + \beta_1 V_{\text{esc}} + \lg(\hat{p}_i)$	103.91	0.063	NB	

Here, in order to further briefly compare the difference between the results of the two samples in the estimated counts of pulsars for all GCs in the Milky Way, we used the optimal model with only one intercept term for further analysis since the estimated detection probabilities of pulsars in some GCs were not available. We therefore adopted the second model (Model no. 2 in the lower section of Table 3), with an AIC value of 103.88, and in which  $\beta_0 = 0.369$  and  $\beta_1 = 0.087$ , for further study. The association from the selected model is significant with a  $P$ -value<sup>12</sup> of  $5.94 \times 10^{-6} < 0.05$ . This provides further support for the potential correlation between the population of pulsars in GCs and their escape velocities. For the sake of brevity (i.e., only one intercept term), the third model from the sample of all GCs was used for further comparisons with the selected model from the FAST sky. The association of the selected model from all GCs is also significant with a  $P$ -value of  $1.78 \times 10^{-7}$  ( $\beta_0 = -0.169$ ,  $\beta_1 = 0.086$ , and  $\text{AIC}=314.60$ ). Assuming that the correlation from the GCs within the FAST is applicable to Galactic GCs outside of the FAST sky, the pulsar numbers of these GCs were estimated accordingly (see Figure 2 and Table 5). As seen in Figure 2, the estimated counts between the FAST sky model and all sky model are slightly different, which may be due to the higher pulsar detection rate in GCs from the FAST (e.g., Yin et al. 2023).

The fact that GCs with larger total mass also have, on average, larger escape velocities is a natural correlation. The  $V_{\text{esc}}$  was derived from the best-fitting N-body models of each GC in Baumgardt’s list, which can be estimated by  $V_{\text{esc}} = \sqrt{2GM/r_{\text{h},1}}$  or  $V_{\text{esc}} = \sqrt{1.5GM/r_{\text{h},\text{m}}}$ , where  $M$ ,  $r_{\text{h},1}$ , and  $r_{\text{h},\text{m}}$  are the GC mass, projected half-light radius, and half-mass radius (3D), respectively. Because neutron stars receive a high natal kick velocity (e.g., Hobbs et al. 2005) it was generally predicted that they would not be retained within GCs, and therefore those within GCs have been proposed to form through a low-velocity channel (e.g., electron-capture supernovae, Ivanova et al. 2008; Freire 2013). Assuming that the evolutionary nature of Galactic GCs are alike, simply the

<sup>12</sup> The probability,  $P$ -value, is a measure of evidence against the null hypothesis in favor of the alternative hypothesis, i.e., a smaller  $P$ -value indicates more significant the correlation between the parameter  $V_{\text{esc}}$  and  $\hat{N}_{\text{psr}}$  (see Turk & Lorimer 2013 and reference therein for details).

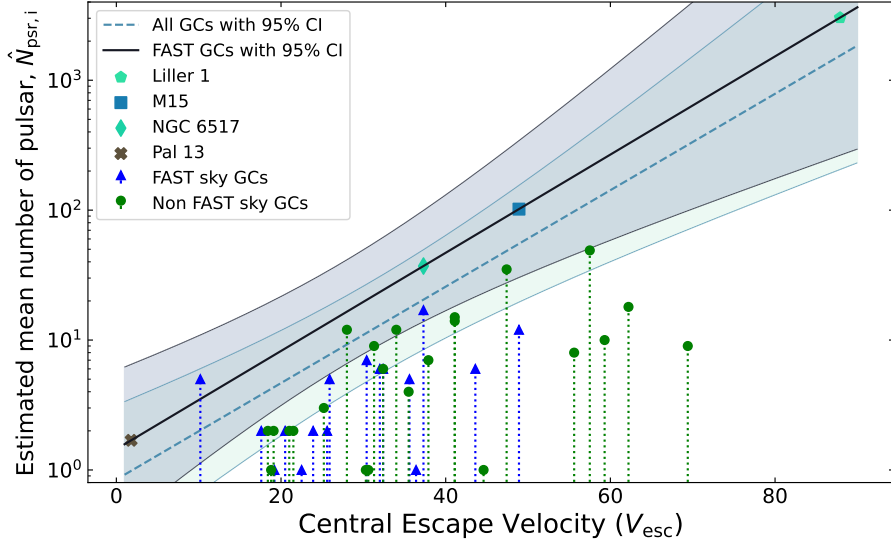


**Figure 2.** The correlation between the number of pulsars and the central escape velocity of Galactic GCs. The lines with 95% credible interval (CI) in grey colour shows the relation between the escape velocity and the number of estimated pulsars, while the stem plot shows the escape velocity of 39 GCs with known pulsars and the number of known pulsars in them. The blue dotted line and the black solid line present the model derived from all GCs and only GCs within FAST sky, respectively. GLIMPSE-C01 (with 6 known pulsars) was not included in the figure as its escape velocity was not available. In the sample, Pal 13 and M15 are the minimum and maximum escape velocities in the FAST sky, respectively. Liller 1 has the largest escape velocity in the Galactic GCs.

total mass of the GCs may influence the number of neutron stars originally retained, as pointed out by [Ransom \(2008\)](#). Therefore, more initial neutron stars can be formed due to a larger cluster mass, while a sufficiently high escape velocity of the cluster considerably ensures retention of the neutron stars in this stage (e.g., [Ivanova et al. 2008](#)). After retention, the initial neutron stars may be recycled to millisecond spin periods by accretion. The escape velocity of cluster is related to the total mass and size of the cluster (i.e. related to density). Higher central density of GC leads to an increase in the formation of more low-mass X-ray binaries and their offspring of millisecond pulsars through close stellar encounters (e.g., [Alpar et al. 1982](#); [Pooley et al. 2003](#)). The dependence here between the number of pulsars and the escape velocity is consistent with previous N-body simulation works exploring the formation of millisecond pulsars in GCs (e.g., [Ivanova et al. 2008](#); [Ye et al. 2019](#)).

The range of  $V_{\text{esc}}$  of the 31 GCs in the FAST sky is  $1.8 \text{ km s}^{-1}$  (Pal 13) to  $48.9 \text{ km s}^{-1}$  (M15). In Table 4 the results of our pulsar number predictions, and those from [Turk & Lorimer \(2013\)](#) are given in order of descending  $V_{\text{esc}}$ . Thus, in the FAST sky M15 (13 pulsars, M15A to M) was expected to host 102 pulsars, being the GC with the largest number of predicted pulsars. Predicted to host 64 pulsars and with at least 6 pulsars discovered by FAST (e.g., [Pan et al. 2021b](#)), M2 is suggested to be the GC with the second largest number of pulsars. With only one pulsar, an eclipsing redback namely M92A, discovered in 2017 by FAST ([Pan et al. 2020](#)), the modeled pulsar number for M92 is 34. Thus, we suggest that more pulsars should be discovered in M92. On the other hand, the possible reasons of missing pulsars can be either the relatively low fluxes and or compact orbits. The only exception is M71. There are 5 pulsars in it, while the modeled pulsar number is 4.

With the  $V_{\text{esc}}$  of  $87.9 \text{ km s}^{-1}$ , Liller 1 is predicted to host thousands of pulsars. The prediction is supported by the previous estimation that it could host  $410_{-210}^{+480}$  pulsars (Abdo et al. 2010; Tam et al. 2011) due to its highest  $\gamma$ -ray luminosity among all GCs. The distance of this GC from the Sun is 8.2 kpc, close enough for finding new pulsars. Located in the bulge of the Milky Way, the heavy dispersive smearing and scatter broadening caused by possible high DM values (e.g.,  $\sim 697 \text{ cm}^{-3} \text{ pc}$  from NE2001, Cordes & Lazio 2002;  $\sim 1104 \text{ cm}^{-3} \text{ pc}$  from YMW16, Yao et al. 2017) can be the reason for missing pulsars. The pulsars in this GC might require higher frequency bands at large radio telescopes.

M54, NGC 6388, NGC 2808, and M75 are the other four GCs with similar or higher  $V_{\text{esc}}$  than M15, but with few pulsars detected. M54 and M75 are located more than 20 kpc away, further than M53 which is the furthest GC with known pulsars. The distance to either NGC 6388 or NGC 2808 is around 10 kpc, similar to Liller1. So, we suggest that the priority of pulsar surveys towards NGC 6388 and NGC 2808 should be higher than those to M54 and M75.

We caution against directly applying the above estimated numbers, as selection bias may still exist and a further analysis is required to refine this simulation. The flux density limit used here (Boyles et al. 2011), as discussed in Turk & Lorimer (2013), is strictly applicable only to long-period pulsars, and thus we focus here on the potential correlation between the pulsar population of GCs and their physical parameters, without analyzing the pulsar detection probability. The updating of some of those numbers may refine the analysis. On the premise that almost all GCs within the FAST sky have been deeply searched for pulsars at the same sensitivity limit, we assume that the population of pulsars within these GCs is more akin to the native population, but a selection bias may still exist by using only these GCs as a sample to estimate the whole Galactic population distribution. For example, most GCs are located around the Galactic center or in the Southern sky, where some of them host the largest number of pulsars, while the GCs within the FAST sky are mostly out of the Galactic plane. Also, most GCs in the FAST sky have smaller amounts of DM and scattering, enabling the initial pulsars within them to be more easily detected. Similarly, the slight difference between the estimated counts derived from the FAST sky and all sky may also arise from the different ranges of cluster physics parameters, such as escape velocities.

In the FAST sky, around 50 GC pulsars were discovered by either FAST (e.g., Pan et al. 2021b) or others (e.g., Glimpse C01 A, McCarver et al. 2023). With known pulsars, the computational time cost for dedispersion can be largely saved. Thus, those GCs with known pulsars should be prioritized for future observing campaigns. After searching for almost all the GCs in FAST sky, 20 pulsars were discovered in the GCs with no previously known pulsars, including M92, M14, M2, NGC 6712, M10, and M12. The probability of pulsar discoveries in GCs with or without known pulsars may not differ significantly. On the other hand, short observations should be carried out before longer ones to reduce unnecessary processing time and to improve chances of finding compact binaries. Based on predictions made here, there is little doubt that the ongoing and future GC pulsar surveys with GMRT (e.g., Gautam et al. 2022), Parkes (e.g., Zhang et al. 2022), MeerKAT (e.g., Ridolfi et al. 2021), and SKA (Hessels et al. 2015) in the near future will bring more discoveries.

## 5. CONCLUSIONS

In this study of FAST observations of NGC 6517, we have reached the following conclusions:

1. Eight new isolated millisecond pulsars, namely PSR J1801–0857K to R, or, NGC 6517K to R, were discovered in NGC 6517. Up to the end of 2023, there are 17 pulsars detected in NGC 6517.
2. NGC 6517J is proven to be a harmonic of NGC 6517B. The phase-connected timing solutions of NGC 6517K to O were obtained. The timing solutions of previously known pulsars were updated and are consistent with previous works.
3. In the framework of the empirical Bayesian model used in this paper, the recently observed sample of GC pulsars favored a correlation between the number of potential pulsars and the central escape velocities unlike the original prediction of Turk & Lorimer (2013) using the same method which predicted the stellar encounter rate as the main factor.
4. In the FAST sky, M2 and M92 may have more pulsars. Outside of the FAST sky, Liller 1, NGC 6388, NGC 2808, M54, and M75 have the highest possibilities for finding new pulsars.

This work is supported by National SKA Program of China (No. 2020SKA0120100), the Basic Science Center Project of the National Nature Science Foundation of China (NSFC) under Grant Nos. 11703047, 11773041, U1931128, U2031119, 12003047 and 12173053. Lei Qian is supported by the Youth Innovation Promotion Association of CAS (id. 2018075, Y2022027), and the CAS “Light of West China” Program. RPE is supported by the Chinese Academy of Sciences President’s International Fellowship Initiative, Grant No. 2021FSM0004. M.L. is supported by Guizhou Provincial Basic Research Program (Natural Science) (ZK[2023] 039), Key Technology R&D Program([2023] 352) and National Natural Science Foundation of China under Grand No. 12363010. This work made use of the data from FAST (Five-hundred-meter Aperture Spherical radio Telescope). FAST is a Chinese national mega-science facility, operated by National Astronomical Observatories, Chinese Academy of Sciences. This work is also supported by the International Centre of Supernovae, Yunnan Key Laboratory (No. 202302AN360001 and 202302AN36000104). Finally, we thank the anonymous referees for their helpful suggestions to bring clarity to the text.

## REFERENCES

- Abdo, A. A., Ackermann, M., Ajello, M., et al. 2009, *Science*, 325, 848, doi: [10.1126/science.1176113](https://doi.org/10.1126/science.1176113)
- . 2010, *A&A*, 524, A75, doi: [10.1051/0004-6361/201014458](https://doi.org/10.1051/0004-6361/201014458)
- Alpar, M. A., Cheng, A. F., Ruderman, M. A., & Shaham, J. 1982, *Nature*, 300, 728, doi: [10.1038/300728a0](https://doi.org/10.1038/300728a0)
- Anderson, S. B., Gorham, P. W., Kulkarni, S. R., Prince, T. A., & Wolszczan, A. 1990, *Nature*, 346, 42, doi: [10.1038/346042a0](https://doi.org/10.1038/346042a0)
- Bahramian, A., Heinke, C. O., Sivakoff, G. R., & Gladstone, J. C. 2013, *ApJ*, 766, 136, doi: [10.1088/0004-637X/766/2/136](https://doi.org/10.1088/0004-637X/766/2/136)
- Barr, E. D., Dutta, A., Freire, P. C. C., et al. 2024, *Science*, 383, 275, doi: [10.1126/science.adg3005](https://doi.org/10.1126/science.adg3005)
- Blandford, R., & Teukolsky, S. A. 1976, *ApJ*, 205, 580, doi: [10.1086/154315](https://doi.org/10.1086/154315)
- Boyles, J., Lorimer, D. R., Turk, P. J., et al. 2011, *ApJ*, 742, 51, doi: [10.1088/0004-637X/742/1/51](https://doi.org/10.1088/0004-637X/742/1/51)
- Burnham, K. P., & Anderson, D. R. 2004, A practical information-theoretic approach, 2
- Camilo, F., & Rasio, F. A. 2005, in *Astronomical Society of the Pacific Conference Series*, Vol. 328, Binary Radio Pulsars, ed. F. A. Rasio & I. H. Stairs, 147, doi: [10.48550/arXiv.astro-ph/0501226](https://doi.org/10.48550/arXiv.astro-ph/0501226)

- Cordes, J. M., & Lazio, T. J. W. 2002, arXiv e-prints, astro, doi: [10.48550/arXiv.astro-ph/0207156](https://doi.org/10.48550/arXiv.astro-ph/0207156)
- Davies, M. B., Benz, W., & Hills, J. G. 1992, *ApJ*, 401, 246, doi: [10.1086/172056](https://doi.org/10.1086/172056)
- Freire, P. C. C. 2013, in *Neutron Stars and Pulsars: Challenges and Opportunities after 80 years*, ed. J. van Leeuwen, Vol. 291, 243–250, doi: [10.1017/S1743921312023770](https://doi.org/10.1017/S1743921312023770)
- Freire, P. C. C., Hessels, J. W. T., Nice, D. J., et al. 2005, *ApJ*, 621, 959, doi: [10.1086/427748](https://doi.org/10.1086/427748)
- Freire, P. C. C., & Ridolfi, A. 2018, *MNRAS*, 476, 4794, doi: [10.1093/mnras/sty524](https://doi.org/10.1093/mnras/sty524)
- Gautam, T., Ridolfi, A., Freire, P. C. C., et al. 2022, *A&A*, 664, A54, doi: [10.1051/0004-6361/202243062](https://doi.org/10.1051/0004-6361/202243062)
- Harris, W. E. 1996, *AJ*, 112, 1487, doi: [10.1086/118116](https://doi.org/10.1086/118116)
- Hessels, J., Possenti, A., Bailes, M., et al. 2015, in *Advancing Astrophysics with the Square Kilometre Array (AASKA14)*, 47, doi: [10.22323/1.215.0047](https://doi.org/10.22323/1.215.0047)
- Hessels, J. W. T., Ransom, S. M., Stairs, I. H., Kaspi, V. M., & Freire, P. C. C. 2007, *ApJ*, 670, 363, doi: [10.1086/521780](https://doi.org/10.1086/521780)
- Hobbs, G., Lorimer, D. R., Lyne, A. G., & Kramer, M. 2005, *MNRAS*, 360, 974, doi: [10.1111/j.1365-2966.2005.09087.x](https://doi.org/10.1111/j.1365-2966.2005.09087.x)
- Hotan, A. W., van Straten, W., & Manchester, R. N. 2004, *PASA*, 21, 302, doi: [10.1071/AS04022](https://doi.org/10.1071/AS04022)
- Ivanova, N., Heinke, C. O., Rasio, F. A., Belczynski, K., & Fregeau, J. M. 2008, *MNRAS*, 386, 553, doi: [10.1111/j.1365-2966.2008.13064.x](https://doi.org/10.1111/j.1365-2966.2008.13064.x)
- Jonas, J., & MeerKAT Team. 2016, in *MeerKAT Science: On the Pathway to the SKA*, 1, doi: [10.22323/1.277.0001](https://doi.org/10.22323/1.277.0001)
- King, A. R., Pringle, J. E., & Wickramasinghe, D. T. 2001, *MNRAS*, 320, L45, doi: [10.1046/j.1365-8711.2001.04184.x](https://doi.org/10.1046/j.1365-8711.2001.04184.x)
- Kremer, K., Fuller, J., Piro, A. L., & Ransom, S. M. 2023, *MNRAS*, 525, L22, doi: [10.1093/mnras/rlad088](https://doi.org/10.1093/mnras/rlad088)
- Kremer, K., Ye, C. S., Kiroğlu, F., et al. 2022, *ApJL*, 934, L1, doi: [10.3847/2041-8213/ac7ec4](https://doi.org/10.3847/2041-8213/ac7ec4)
- Lynch, R. S., Ransom, S. M., Freire, P. C. C., & Stairs, I. H. 2011, *ApJ*, 734, 89, doi: [10.1088/0004-637X/734/2/89](https://doi.org/10.1088/0004-637X/734/2/89)
- Lyne, A. G., Brinklow, A., Middleditch, J., Kulkarni, S. R., & Backer, D. C. 1987, *Nature*, 328, 399, doi: [10.1038/328399a0](https://doi.org/10.1038/328399a0)
- Manchester, R. N., Hobbs, G. B., Teoh, A., & Hobbs, M. 2005, *AJ*, 129, 1993, doi: [10.1086/428488](https://doi.org/10.1086/428488)
- McCarver, A. V., Maccarone, T. J., Ransom, S. M., et al. 2023, arXiv e-prints, arXiv:2312.11694, doi: [10.48550/arXiv.2312.11694](https://doi.org/10.48550/arXiv.2312.11694)
- Nan, R., Li, D., Jin, C., et al. 2011, *International Journal of Modern Physics D*, 20, 989, doi: [10.1142/S0218271811019335](https://doi.org/10.1142/S0218271811019335)
- Nice, D., Demorest, P., Stairs, I., et al. 2015, *Tempo: Pulsar timing data analysis*, Astrophysics Source Code Library, record ascl:1509.002. <http://ascl.net/1509.002>
- Pan, Z., Ransom, S. M., Lorimer, D. R., et al. 2020, *ApJL*, 892, L6, doi: [10.3847/2041-8213/ab799d](https://doi.org/10.3847/2041-8213/ab799d)
- Pan, Z., Ma, X.-Y., Qian, L., et al. 2021a, *Research in Astronomy and Astrophysics*, 21, 143, doi: [10.1088/1674-4527/21/6/143](https://doi.org/10.1088/1674-4527/21/6/143)
- Pan, Z., Qian, L., Ma, X., et al. 2021b, *ApJL*, 915, L28, doi: [10.3847/2041-8213/ac0bbd](https://doi.org/10.3847/2041-8213/ac0bbd)
- Pan, Z., Lu, J. G., Jiang, P., et al. 2023, *Nature*, 620, 961, doi: [10.1038/s41586-023-06308-w](https://doi.org/10.1038/s41586-023-06308-w)
- Pooley, D., Lewin, W. H. G., Anderson, S. F., et al. 2003, *ApJL*, 591, L131, doi: [10.1086/377074](https://doi.org/10.1086/377074)
- Qian, L., Yao, R., Sun, J., et al. 2020, *The Innovation*, 1, 100053, doi: [10.1016/j.xinn.2020.100053](https://doi.org/10.1016/j.xinn.2020.100053)
- Ransom, S. M. 2001, PhD thesis, Harvard University, Massachusetts
- Ransom, S. M. 2008, in *American Institute of Physics Conference Series*, Vol. 983, 40 Years of Pulsars: Millisecond Pulsars, Magnetars and More, ed. C. Bassa, Z. Wang, A. Cumming, & V. M. Kaspi, 415–423, doi: [10.1063/1.2900267](https://doi.org/10.1063/1.2900267)
- Ransom, S. M., Eikenberry, S. S., & Middleditch, J. 2002, *AJ*, 124, 1788, doi: [10.1086/342285](https://doi.org/10.1086/342285)
- Ransom, S. M., Hessels, J. W. T., Stairs, I. H., et al. 2005, *Science*, 307, 892, doi: [10.1126/science.1108632](https://doi.org/10.1126/science.1108632)
- Ridolfi, A., Gautam, T., Freire, P. C. C., et al. 2021, *MNRAS*, 504, 1407, doi: [10.1093/mnras/stab790](https://doi.org/10.1093/mnras/stab790)

- Robinson, C., Lyne, A. G., Manchester, R. N., et al. 1995, *MNRAS*, 274, 547, doi: [10.1093/mnras/274.2.547](https://doi.org/10.1093/mnras/274.2.547)
- Schwab, J. 2021, *ApJ*, 906, 53, doi: [10.3847/1538-4357/abc87e](https://doi.org/10.3847/1538-4357/abc87e)
- Sigurdsson, S., Richer, H. B., Hansen, B. M., Stairs, I. H., & Thorsett, S. E. 2003, *Science*, 301, 193, doi: [10.1126/science.1086326](https://doi.org/10.1126/science.1086326)
- Tam, P. H. T., Kong, A. K. H., Hui, C. Y., et al. 2011, *ApJ*, 729, 90, doi: [10.1088/0004-637X/729/2/90](https://doi.org/10.1088/0004-637X/729/2/90)
- Turk, P. J., & Lorimer, D. R. 2013, *MNRAS*, 436, 3720, doi: [10.1093/mnras/stt1850](https://doi.org/10.1093/mnras/stt1850)
- Verbunt, F., & Freire, P. C. C. 2014, *A&A*, 561, A11, doi: [10.1051/0004-6361/201321177](https://doi.org/10.1051/0004-6361/201321177)
- Wu, Y., Pan, Z., Qian, L., et al. 2023, arXiv e-prints, arXiv:2312.06067, doi: [10.48550/arXiv.2312.06067](https://doi.org/10.48550/arXiv.2312.06067)
- Yao, J. M., Manchester, R. N., & Wang, N. 2017, *ApJ*, 835, 29, doi: [10.3847/1538-4357/835/1/29](https://doi.org/10.3847/1538-4357/835/1/29)
- Ye, C. S., Kremer, K., Chatterjee, S., Rodriguez, C. L., & Rasio, F. A. 2019, *ApJ*, 877, 122, doi: [10.3847/1538-4357/ab1b21](https://doi.org/10.3847/1538-4357/ab1b21)
- Ye, C. S., Kremer, K., Ransom, S. M., & Rasio, F. A. 2024, *ApJ*, 961, 98, doi: [10.3847/1538-4357/ad089a](https://doi.org/10.3847/1538-4357/ad089a)
- Yin, D.-J., Zhang, L.-Y., Li, B.-D., et al. 2023, *Research in Astronomy and Astrophysics*, 23, 055012, doi: [10.1088/1674-4527/acc37e](https://doi.org/10.1088/1674-4527/acc37e)
- Zhang, L., Ridolfi, A., Blumer, H., et al. 2022, *ApJL*, 934, L21, doi: [10.3847/2041-8213/ac81c3](https://doi.org/10.3847/2041-8213/ac81c3)
- Zhao, J., & Heinke, C. O. 2022, *MNRAS*, 511, 5964, doi: [10.1093/mnras/stac442](https://doi.org/10.1093/mnras/stac442)



**Table 4.** The 45 GCs in FAST sky. The latest central escape velocities ( $V_{\text{esc}}$ ) of GCs are from the Baumgardt’s list (The 4<sup>th</sup> Mar. 2023) version<sup>14</sup>), while other physical parameters of GCs are the same as in Turk & Lorimer (2013). The  $N_{\text{obs}}$  is the number of observed known pulsars by the end of 2023. The expected number of potential pulsars of  $\hat{N}_{\text{psr},1}$  and  $\hat{N}_{\text{psr},2}$  are from the Equation 13 ( $\ln \hat{\lambda} = -1.1 + 1.5 \lg \Gamma$ ) of Turk & Lorimer (2013) and model no. 2 from the FAST sky only sample in this work ( $\ln \hat{N}_{\text{psr},i} = 0.369 + 0.087 V_{\text{esc},i}$ ), respectively. The  $D_{\text{Sun}}$  is the distance from the Sun (Harris 1996, 2010 edition). The  $L_{\text{min}}$  ( $L_{\text{min},i} = S_{\text{min},i} D_{\text{Sun},i}^2$ , Boyles et al. 2011) is from the list of flux density detection limits of GCs. Note: Table 4 and Table 5 are also can be presented in an online available form.

ID	Name	$D_{\text{Sun}}$ (kpc)	$L_{\text{min}}$ (mJy kpc <sup>2</sup> )	$\Gamma$	$V_{\text{esc}}$ (km s <sup>-1</sup> )	$N_{\text{obs}}$	$\hat{N}_{\text{psr},1}$	$R_1$ ( $N_{\text{obs}}/\hat{N}_{\text{psr},1}$ )	$\hat{N}_{\text{psr},2}$	$R_2$ ( $N_{\text{obs}}/\hat{N}_{\text{psr},2}$ )
NGC 7078	M 15	10.4	2.2714	4510	48.9	12	80	0.15	102	0.12
NGC 7089	M 2	11.5	0.7935	518	43.6	6	20	0.3	64	0.09
NGC 6517		10.6	0.3371	338	37.3	17	15	1.13	37	0.46
NGC 6341	M 92	8.3	0.3513	270	36.4	1	13	0.08	34	0.03
NGC 6402	M 14	9.3	4.7397	124	35.6	5	8	0.63	32	0.16
NGC 6205	M 13	7.1	1.3611	68.9	32.4	6	5	1.2	24	0.25
NGC 5272	M 3	10.2	2.1848	194	32	6	10	0.6	23	0.26
NGC 5904	M 5	7.5	1.4063	164	30.4	7	9	0.78	20	0.35
NGC 5024	M 53	17.9	6.0878	35.4	25.9	5	3	1.67	14	0.36
NGC 6760		7.4	2.0261	56.9	25.6	2	5	0.4	13	0.15
NGC 6229		30.5		47.6	25.3		4	0	13	0
NGC 5634		25.2		20.2	24.2		2	0	12	0
NGC 6254	M 10	4.4	1.2894	31.4	23.9	2	3	0.67	12	0.17
NGC 6539		7.8	2.8595	42.1	22.5	1	4	0.25	10	0.1
NGC 6779	M 56	9.4	2.209	27.7	21.9		3	0	10	0
NGC 6934		15.6	6.8141	29.9	21.4		3	0	9	0
NGC 6749		7.9	1.9971	38.5	20.5	2	4	0.5	9	0.22
NGC 6712		6.9	0.319	30.8	19.2	1	3	0.33	8	0.13
Pal 2		27.2	25.1546	929	19.2		29	0	8	0
NGC 2419		82.6		2.8	18.2		1	0	7	0
NGC 6218	M 12	4.8	1.2626	13	17.6	2	2	1	7	0.29
NGC 6171	M 107	6.4	2.2446	6.77	15.7		1	0	6	0
NGC 7006		41.2	32.2514	9.4	15.7		1	0	6	0
Pal 10		5.9	0.8006	59	14.6		5	0	5	0
IC 1276	Pal 7	5.4		7.97	14.3		1	0	5	0
NGC 4147		19.3	7.0773	16.6	14.2		2	0	5	0

Continued on next page

**Table 4 – continued from previous page**

ID	Name	$D_{\text{Sun}}$ (kpc)	$L_{\text{min}}$ (mJy kpc <sup>2</sup> )	$\Gamma$	$V_{\text{esc}}$ (km s <sup>-1</sup> )	$N_{\text{obs}}$	$\hat{N}_{\text{psr},1}$	$R_1$ ( $N_{\text{obs}}/\hat{N}_{\text{psr},1}$ )	$\hat{N}_{\text{psr},2}$	$R_2$ ( $N_{\text{obs}}/\hat{N}_{\text{psr},2}$ )
NGC 6981	M 72	17	1.734	4.69	12.4		1	0	4	0
NGC 6426		20.6	10.609	1.58	10.3		0	-	4	0
NGC 6535		6.8	1.8958	0.388	10.2		0	-	4	0
NGC 6838	M 71	4	0.304	2.05	10.2	5	1	5	4	1.25
NGC 6366		3.5		5.14	9.1		1	0	3	0
IC 1257		25			6.7		-	-	3	0
NGC 5466		16	5.632	0.239	6.5		0	-	3	0
NGC 5053		17.4	6.0552	0.105	6		0	-	2	0
Pal 15		45.1	77.2924	0.0222	4.3		0	-	2	0
Pal 11		13.4		20.8	4		2	0	2	0
Pal 4		108.7		0.0189	2.6		0	-	2	0
Pal 3		92.5		0.0409	2.4		0	-	2	0
Pal 14	AvdB	76.5		0.00186	2.3		0	-	2	0
Pal 5		23.2	17.2237	0.00212	2.1		0	-	2	0
Pal 13		26	14.196	0.00109	1.8		0	-	2	0
Whiting 1		30.1			1.1		-	-	2	0
GLIMPSE01		4.2				2	-	-	-	-
Ko 1		48.3					-	-	-	-
Ko 2		34.7					-	-	-	-

**Table 5.** The 112 GCs outside of FAST aky

ID	Name	$D_{\text{Sun}}$ (kpc)	$L_{\text{min}}$ (mJy kpc <sup>2</sup> )	$\Gamma$	$V_{\text{esc}}$ (km s <sup>-1</sup> )	$N_{\text{obs}}$	$\hat{N}_{\text{psr},1}$	$R_1$ ( $N_{\text{obs}}/\hat{N}_{\text{psr},1}$ )	$\hat{N}_{\text{psr},2}$	$R_2$ ( $N_{\text{obs}}/\hat{N}_{\text{psr},2}$ )
Liller 1		8.2	0.6657	391	87.9		16	0	3030	0
NGC 6441		11.6	1.6685	2300	69.4	9	52	0.17	606	0.01
NGC 6715	M 54	26.5		2520	68.9		55	0	580	0
NGC 5139	$\omega$ -Cen	5.2	1.306	90.4	62.2	18	6	3	324	0.06
NGC 6388		9.9	5.3709	899	60		28	0	267	0
NGC 6266	M 62	6.8	1.0219	1670	59.3	10	42	0.24	252	0.04
Terzan 5	Terzan 11	6.9	0.5523	6800	57.5	49	104	0.47	215	0.23
NGC 6440		8.5	0.7081	1400	55.6	8	37	0.22	182	0.04
NGC 2808		9.6	5.0504	923	53.1		28	0	147	0
NGC 6864	M 75	20.9		307	48.4		14	0	97	0
NGC 104	47 Tuc	4.5	3.3939	1000	47.4	35	30	1.17	89	0.39
NGC 6139		10.1	7.9058	307	46.4		14	0	82	0
NGC 5824		32.1		984	44.8		30	0	71	0
NGC 6273	M 19	8.8	4.2437	200	44.8		11	0	71	0

Continued on next page

Table 5 – continued from previous page

ID	Name	$D_{\text{Sun}}$ (kpc)	$L_{\text{min}}$ (mJy kpc <sup>2</sup> )	$\Gamma$	$V_{\text{esc}}$ (km s <sup>-1</sup> )	$N_{\text{obs}}$	$\hat{N}_{\text{psr},1}$	$R_1$ ( $N_{\text{obs}}/\hat{N}_{\text{psr},1}$ )	$\hat{N}_{\text{psr},2}$	$R_2$ ( $N_{\text{obs}}/\hat{N}_{\text{psr},2}$ )
NGC 6093	M 80	10	0.57	532	44.6	1	20	0.05	70	0.01
NGC 5286		11.7	7.5016	458	41.8		18	0	55	0
NGC 1851		12.1	4.4069	1530	41.1	15	40	0.38	52	0.29
NGC 6626	M 28	5.5	0.124	648	41.1	14	23	0.61	52	0.27
Terzan 1	HP 2	6.7	3.479	0.292	37.9	7	0	-	39	0.18
NGC 6541		7.5	0.54	386	37.3		16	0	37	0
NGC 6656	M 22	3.2	0.0584	77.5	35.5	4	6	0.67	32	0.13
Terzan 10		5.8		4430	35.2		79	0	31	0
NGC 362		8.6		735	34	12	25	0.48	28	0.43
NGC 5694		35		191	33.6		10	0	27	0
NGC 6553		6		69	32.8		5	0	25	0
NGC 6522		7.7	3.2491	363	32.4	6	15	0.4	24	0.25
NGC 6333	M 9	7.9	3.4201	131	32.4		8	0	24	0
NGC 6380	Ton 1	10.9		116	31.8		7	0	23	0
NGC 6752		4	0.504	401	31.3	9	17	0.53	22	0.41
NGC 6356		15.1		88.1	31.1		6	0	22	0
NGC 5986		10.4	0.4002	61.9	30.6	1	5	0.2	21	0.05
NGC 6316		10.4		77	30.3	1	6	0.17	20	0.05
Terzan 9		7.1		1.71	29.1		0	-	18	0
NGC 6569		10.9		53.6	28.4		4	0	17	0
NGC 6624		7.9	0.9986	1150	28	12	33	0.36	17	0.71
NGC 6453		11.6	10.8186	371	27.9		16	0	16	0
NGC 6284		15.3	12.8281	666	27.6		23	0	16	0
NGC 1904	M 79	12.9		116	27.6		7	0	16	0
NGC 6293		9.5	4.9457	847	27.4		27	0	16	0
NGC 6287		9.4	6.8479	36.3	26.8		3	0	15	0
NGC 6638		9.4		137	26.7		8	0	15	0
Terzan 6	HP 5	6.8	0.3376	2470	26.4		54	0	14	0
NGC 6681	M 70	9	6.2775	1040	25.3		31	0	13	0
NGC 5927		7.7	3.2491	68.2	25.2		5	0	13	0
NGC 6544		3	0.3492	111	25.2	3	7	0.43	13	0.23
NGC 5946		10.6	6.1573	134	24.3		8	0	12	0
NGC 6637	M 69	8.8		89.9	24.3		6	0	12	0
NGC 6401		10.6	8.7079	44	23.6		4	0	11	0
Terzan 4	HP 4	7.2			23.1		-	-	11	0
NGC 6304		5.9	1.9076	123	22.8		8	0	11	0
NGC 4833		6.6	3.3759	25	22.2		3	0	10	0
FSR 1735		9.8			22.2		-	-	10	0

Continued on next page

Table 5 – continued from previous page

ID	Name	$D_{\text{Sun}}$ (kpc)	$L_{\text{min}}$ (mJy kpc <sup>2</sup> )	$\Gamma$	$V_{\text{esc}}$ (km s <sup>-1</sup> )	$N_{\text{obs}}$	$\hat{N}_{\text{psr},1}$	$R_1$ ( $N_{\text{obs}}/\hat{N}_{\text{psr},1}$ )	$\hat{N}_{\text{psr},2}$	$R_2$ ( $N_{\text{obs}}/\hat{N}_{\text{psr},2}$ )
NGC 6355		9.2	6.5596	99.2	21.6		7	0	9	0
NGC 6397		2.3	0.1666	84.1	21.5	2	6	0.33	9	0.22
NGC 6723		8.7	4.1478	11.4	21.5		2	0	9	0
NGC 1261		16.3	10.3088	15.4	21.4		2	0	9	0
NGC 7099	M 30	8.1	0.7086	324	21	2	14	0.14	9	0.22
NGC 6325		7.8	3.334	118	20.6		7	0	9	0
HP 1	BH 229	8.2		0.662	20.3		0	-	8	0
NGC 6642		8.1	3.5954	97.8	20		7	0	8	0
NGC 6256		10.3		169	19.8		9	0	8	0
Pal 6		5.8	0.2254	15.5	19.7		2	0	8	0
NGC 6652		10	7.75	700	19.1	2	24	0.08	8	0.25
NGC 6528		7.9	3.4201	278	19		13	0	8	0
NGC 6121	M 4	2.2	0.636	26.9	18.8	1	3	0.33	7	0.14
NGC 6342		8.5	19.5075	44.8	18.4	2	4	0.5	7	0.29
NGC 6809	M 55	5.4	2.2599	3.23	18.1		1	0	7	0
Terzan 2	HP 3	7.5		22.1	17.4		3	0	7	0
NGC 3201		4.9	1.3157	7.17	17.3		1	0	7	0
NGC 6584		13.5	9.9873	11.8	16.7		2	0	6	0
NGC 6558		7.4	3.4663	105	16.7		7	0	6	0
UKS 1		7.8	3.334	100	15.7		7	0	6	0
NGC 4372		5.8	1.8435	0.233	15.5		0	-	6	0
NGC 6235		11.5	7.2473	5.75	15.5		1	0	6	0
Djorg 2	ESO456-SC38	6.3		46.4	15.4		4	0	6	0
NGC 2298		10.8	0.4782	4.31	15.3		1	0	5	0
NGC 6540	Djorg 3	5.3	2.177	263	15.1		13	0	5	0
NGC 6144		8.9	4.3407	3.14	15		1	0	5	0
Djorg 1		13.7		9.04	14.8		1	0	5	0
NGC 4590	M 68	10.3	5.8137	5.82	14.8		1	0	5	0
NGC 6352		5.6		6.74	13.2		1	0	5	0
NGC 6362		7.6		4.56	13.1		1	0	5	0
Terzan 12		4.8		35.8	13.1		3	0	5	0
Lynga 7	BH184	8			12.8		-	-	4	0
NGC 5897		12.5	0.8594	0.851	12.5		0	-	4	0
Pal 8		12.8		4.22	11.7		1	0	4	0
Ton 2	Pismis 26	8.2		4.29	11.6		1	0	4	0
NGC 6717	Pal 9	7.1	2.7625	39.8	11.6		4	0	4	0
NGC 6101		15.4		0.974	11.5		0	-	4	0
2MS-GC01	2MASS-GC01	3.6			11.2		-	-	4	0

Continued on next page

Table 5 – continued from previous page

ID	Name	$D_{\text{Sun}}$ (kpc)	$L_{\text{min}}$ (mJy kpc <sup>2</sup> )	$\Gamma$	$V_{\text{esc}}$ (km s <sup>-1</sup> )	$N_{\text{obs}}$	$\hat{N}_{\text{psr},1}$	$R_1$ ( $N_{\text{obs}}/\hat{N}_{\text{psr},1}$ )	$\hat{N}_{\text{psr},2}$	$R_2$ ( $N_{\text{obs}}/\hat{N}_{\text{psr},2}$ )
NGC 288		8.9	0.5149	0.766	10.9	0	-	-	4	0
NGC 6496		11.3	6.9974	0.657	10.8	0	-	-	4	0
IC 4499		18.8		0.797	10.5	0	-	-	4	0
BH 261	AL 3	6.5			9.1	-	-	-	3	0
2MS-GC02	2MASS-GC02	4.9			8.4	-	-	-	3	0
Terzan 3		8.2		0.89	7.6	0	-	-	3	0
ESO-SC06	ESO280-SC06	21.4			6.8	-	-	-	3	0
Terzan 8		26.3		0.0793	6	0	-	-	2	0
Rup 106		21.2		0.359	5.6	0	-	-	2	0
1636-283	ESO452-SC11	8.3		1.72	5.5	0	-	-	2	0
Terzan 7		22.8		1.59	4.6	0	-	-	2	0
Arp 2		28.6		0.00518	4.5	0	-	-	2	0
NGC 7492		26.3		0.192	4.4	0	-	-	2	0
Pyxis		39.4			3.6	-	-	-	2	0
AM 1	E 1	123.3		0.00419	3.3	0	-	-	2	0
Pal 12		19	2.2382	0.397	2.5	0	-	-	2	0
E 3		8.1		0.0759	2.4	0	-	-	2	0
Eridanus		90.1		0.0339	2.2	0	-	-	2	0
Pal 1		11.1		0.895	1.9	0	-	-	2	0
AM 4		32.2		0.0026	0.9	0	-	-	2	0
BH 176		18.9		0.146		0	-	-	-	-
GLIMPSE02		5.5				-	-	-	-	-